# MAGNETIZATION OF SUPERCONDUCTING ALLOY Ti—22 at.%Nb

V. R. KARASIK, N. G. VASIL'EV, and V. G. ERSHOV

P. N. Lebedev Physics Institute, USSR Academy of Sciences

Submitted April 29, 1970

Zh. Eksp. Teor. Fiz. 59, 790—798 (September, 1970)

A modified Bean model is used to show that the concept of the critical state is applicable to a superconducting alloy with a rigidly pinned vortex lattice. The influence of the Pauli paramagnetism on the ratio $H_{c3}/H_{c2}$ near $T_c$ is investigated. The existence of a proximity effect is demonstrated for the alloy Ti—22 at.% Nb containing $\omega$-phase particles.

IN 1962 Bean introduced the concept of the critical state, wherein the current density at each point of the volume of the superconductor is equal to the critical value[1]. For the critical state, it does not matter which mechanism stabilizes the Abrikosov vortex lattice and which method is used to excite the current. In[2], for example, it was shown that when a transport current $J_z$ is introduced in a cylindrical sample, the circular current $J_\varphi$ induced by the magnetic field attenuates and vanishes at $J_z = J_c$. The critical current densities $j_z$, $j_\varphi$, and $j_c$ are then connected by the relation $j_c^2 = j_z^2 + j_\varphi^2$.

In view of the general character of the idea of the critical state, it would be expected to apply to superconducting alloys with rigidly pinned vortex lattices[3], in which destruction of superconductivity by current is connected with attaining of the critical velocity by the superconducting condensate. We have therefore undertaken an investigation of the magnetization of the alloy Ti—22 at.% Nb by induced currents, and its dependence on the temperature, magnetic-field intensity, and sample dimensions. Incidentally, we have measured also the ratio $H_{c3}/H_{c2}$ near $T_c$ and investigated the action of the proximity effect on the dispersed segregations of the $\omega$ phase.

## 1. MEASUREMENT PROCEDURE

The magnetic-field source was the internal section of a superconducting solenoid, described in[4] and graciously furnished to us by V. V. Sychev and V. B. Zenkevich. The homogeneity of the magnetic field in the central region was not worse than 1% over a length of 60 mm. The current constant of the internal section was 2.12 kOe/A. The section was fed from a semiconducting current regulator[15], ensuring a field stability not worse than $10^{-5}$. The magnetization was measured by a ballistic method. We used both differential and summation ballistic coils. The differential coils were placed one inside the other and had an effective turns number $n_1 - n_2 = 11{,}000$. The summation coils were mounted on a common axis and consisted of 15,000 turns each. The coil height was 10 mm, the sample length 14 mm, and the distance between the summing coils 20 mm. The diameter of the winding wire was 20 $\mu$.

The coil system was placed inside a small stainless-steel Dewar covered on the top with a copper plug with a threaded gasket. A tube was soldered inside the plug and served as a guide for a rod carrying the sample. The other end of the tube was secured in a cap. The temperature inside the Dewar was measured with a carbon thermometer calibrated against a standard germanium thermometer. The temperature gradient on the Dewar axis, in the region where the sample moved, did not exceed 0.04°K.

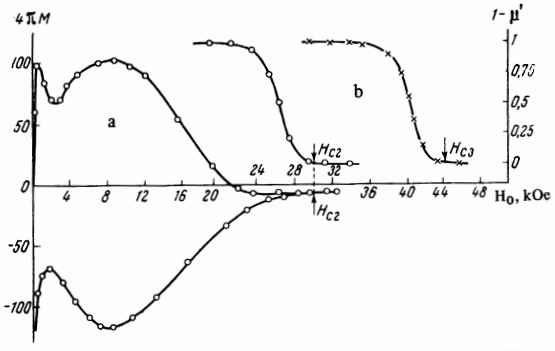


FIG. 1. Method of determining the critical magnetic fields $H_{C2}(T)$ and $H_{C3}(T)$: a—determination of $H_{C2}(T)$ from the magnetization curve; b—determination of $H_{C2}(T)$ and $H_{C3}(T)$ from the real part of the magnetic susceptibility $\mu'$; O—external magnetic field $\mathbf{H}_0$ perpendicular to the sample axis; X—$\mathbf{H}_0$ parallel to the sample axis (sample 5). T = 5.56° K; M and $\mu'$ are in arbitrary units.

The critical surface superconductivity currents $j_{c.\,sur}$ and the values of the magnetic field $H_{C2}$ and $H_{C3}$ were determined from the dependence of the real part of the magnetic susceptibility on the intensity of the external magnetic field[5]. In determining $j_{c.\,sur}$ and $H_{C3}$, the sample and the axis of the measuring, compensation, and modulation coils were placed along the external field $H_0$, and in determining $H_{C2}$ they were placed at an angle 90° to $H_0$. The curves $M(H_0)$ and $1 - \mu' = f(H_0)$, illustrating the foregoing, are shown in Fig. 1[1)].

To obtain temperatures $4.2°K < T \leq T_c$, we used an inverted Dewar with a working channel 8.5 mm. The outside diameter of both systems of coils (for the longitudinal and transverse fields did not exceed 8 mm, and the sample length was half the height of the measuring coils. The samples were cylindrical with radii 0.35—0.1 mm and were prepared at the Moscow Engineering Physics Institute under the direction of Yu. F.

[1)]As shown by control measurements performed at $T > T_c$, the change of sign of $M(H_0)$ as $H_0 \to H_{c2}$ (see Fig. 1) is connected with the weak ferromagnetism of the sample.

Bychkov. The heat-treatment conditions are described in the figure captions.

## 2. MAGNETIC MOMENT OF CIRCULAR CURRENTS INDUCED BY AN EXTERNAL MAGNETIC FIELD

To estimate the applicability of the critical-state hypothesis to an alloy with a rigid vortex lattice, we use the law of variation of the density of the critical transport current $j_{c\perp}(H_0)$, which is known from independent measurements, and calculate the magnetic moment M of the induced currents as a function of the external field $H_0$, after which we compare the calculated value with that determined by experiment.

Calculation of $M(H_0)$ for the case $j_{c\perp}$ = const was carried out by Bean[1]. For the case $j_{c\perp} = A/(H_0 + B_0)$, where A and $B_0$ are constant, the calculation was made by Fietz[6]. In the alloy Ti—22 at.% Nb and in a number of other materials, the change of the critical current satisfies, in a wide range of magnetic fields, the law

$$j_c(H_0) = j_0 \exp\{-H_0/H_{cr}\}, \tag{1}$$

where $j_0$ and $H_{cr}$ are the parameters of the given substance.

We modify Bean's model[1] as applied to (1). To this end, we calculate the magnetic moment per unit length of an infinitely long cylinder of radius R the critical state. Let the external field $H_0$ be directed along the cylinder axis. Then[2)]

$$-\frac{dH}{dr} = -\frac{4\pi}{c} j_0 \exp\left\{-\frac{H_0}{H_{cr}}\right\}. \tag{2}$$

The minus sign in front of $j_0$ indicates that the induced currents have a diamagnetic character. From (2) we obtain the distribution of the current and of the magnetic field along the radius of the cylinder

$$H(r) = H_{cr} \ln\left[\exp\left\{\frac{H_0}{H_{cr}}\right\} - \frac{4\pi}{cH_{cr}} j_0 (R-r)\right], \tag{3}$$

$$j(r) = j_0 \Big/ \left[\exp\left\{\frac{H_0}{H_{cr}}\right\} - \frac{4\pi}{cH_{cr}} j_0 (R-r)\right]. \tag{4}$$

When $0 < r < r_{cr}$, determined from the condition

$$r_{cr} = R + \frac{cH_{cr}}{4\pi j_0}\left(1 - \exp\left\{\frac{H_0}{H_{cr}}\right\}\right), \tag{5}$$

the current in the magnetic field vanish identically.

We proceed to calculate the magnetic moment. Introducing the notation

$$\frac{cH_{cr}}{4\pi j_0 R} = b, \quad \frac{H_0}{H_{cr}} = \alpha, \quad be^{\alpha} = k \tag{6}$$

and using formula (4) and the definition of the magnetic moment

$$M = \frac{1}{c}\int_0^R \pi r^2 j(r)\, dr, \tag{7}$$

we obtain (per unit volume)

$$M = -H_{cr}[\alpha(1-k)^3 + {}^1/_2(k-b)(b+4-3k)] \tag{8}$$

for $0 < r_{cr} < R$ and

$$M = -H_{cr}\left[-(1-k)^2 \ln\left(1-\frac{1}{k}\right) - k + \frac{3}{2}\right] \tag{9}$$

for $r_{cr} = 0$. Formulas (8) and (9) are joined together at the point

$$H_0^* = H_{cr} \ln\left(1 + \frac{1}{b}\right). \tag{10}$$

Then

$$M = -H_{cr}\left[b^2 \ln\left(1+\frac{1}{b}\right) - b + \frac{1}{2}\right]. \tag{11}$$

In weak and strong magnetic fields, the exact solutions can be replaced by approximate ones. Expanding in (8) $e^{\alpha}$ in powers of $\alpha$ and retaining terms up to $\alpha^3$, we obtain

$$M = H_{cr}\left[\alpha^3\left(\frac{b^2}{3} - \frac{2}{3}b\right) - b\alpha^2 + \alpha\right]. \tag{12}$$

In strong magnetic fields, the expansion parameter is $1/ke^{-\alpha}/b$:

$$M = H_{cr}\left[\frac{1}{3b}e^{-\alpha} + \frac{1}{12b^2}e^{-2\alpha} + \frac{1}{30b^3}e^{-3\alpha}\right]. \tag{13}$$

The approximate expressions (12) and (13) describe the curve with good accuracy, with the exception of the region adjacent to the maximum.

Formulas (8) and (9) were obtained under the assumption that the contribution of the equilibrium magnetization and of the surface currents to the magnetic moment can be neglected. The equilibrium magnetization $M_0(H_0)$ reaches its maximum value at the point $H_0 = H_{c1}$. As is well known[7]

$$H_{c1} \approx \frac{H_c}{\varkappa} \ln \varkappa. \tag{14}$$

For our alloy at T = 4.2°K we have $H_c \approx 1200$ Oe, $\kappa \approx 60$, and $H_{c1} \approx 100$ Oe. Since the magnetization connected with the currents amounts to 5—8 kOe, the error due to neglecting $M_0(H_0)$ may turn out to be appreciable only at small values of $H_0$. Measurements of the critical currents of the surface superconductivity of our samples were made in the region $H_{c2} \leq H_0 \leq H_{c3}$. Extrapolation of the results towards weaker fields leads to values $j_{c.\,sur} < 10$ A/cm, corresponding to a magnetization $M_{c.\,sur} < 10$ Oe. Thus, the assumptions made in the derivation of (8) and (9) are perfectly justified.

A consequence of the critical state is a size effect, namely a dependence of the position of the maximum on the $M(H_0)$ curve, corresponding to $r_{cr} = 0$, on the sample radius (see formula (10)). Figure 2 shows the results of the measurements on the magnetization of samples 1, 2, and 3 which differ only in their radii. We see that with increasing radius the maxima shift towards stronger magnetic fields. The quantitative estimates of $H_0^*$ agree with formula (10).

A comparison of the experimental results with formulas (12) and (13) is shown in Fig. 3a (sample 4). The best agreement between the calculated and experimental data is obtained at

$$j_0 = 7.0 \cdot 10^5 \text{ A/cm}^2, \quad H_{cr} = 18.3 \text{ kOe}. \tag{15}$$

Simultaneously, measurements were made, on the same wire from which sample 4 was cut, of the dependence of the critical transport current on the intensity of the perpendicular external field, and, by plotting

$$\ln j_{c\perp}(H_0) = -H_0/H_{cr},$$

it was found that

[2)] A. I. Rusinov took part in the derivation of formulas (2)–(13).

$$j_0 = 6{,}7 \cdot 10^5 \text{ A/cm}^2, \; H_{cr} = 18{,}31 \text{ kOe}. \quad (16)$$

The difference between formulas (15) and (16) lies within the limits of the measurement errors. It can therefore be assumed that the critical-state model is applicable to the case of a rigid vortex lattice.

Figures 4 and 5 demonstrate the correlation between the form of the curves $j_{c\perp}(H_0)$, $j_{c\parallel}(H_0)$, and $M(H_0)$. The $j_{c\perp}(H_0)$ curve shown in Fig. 4b (sample 5) exhibits the "peak effect" connected with the breakdown of the superconductivity of the $\omega$ particles[3]. A similar peak is observed also on the $M(H_0)$ curves (Fig. 4a). The steep decrease of the current in Fig. 4b in weak magnetic fields corresponds to a strictly reproducible decrease of the magnetization to practically zero in Fig. 4a.

Figure 4a shows also a partial hysteresis loop. The curvilinear character of its vertical branches clearly indicates a volume flow of the magnetizing currents. Figure 5 (sample 6) reveals the close connection between the jump of $M(H_0)$ in a field $H_0 \sim 1-1.5$ kOe and the behavior of $j_{c\perp}(H_0)$. An interesting fact is the agreement between the positions of the maxima on the curves $j_{c\parallel}(H_0)$ and $M(H_0)$, resulting from the filling of the cross section with current (compare Figs. 3a with 3b and Figs. 5a with 5b).

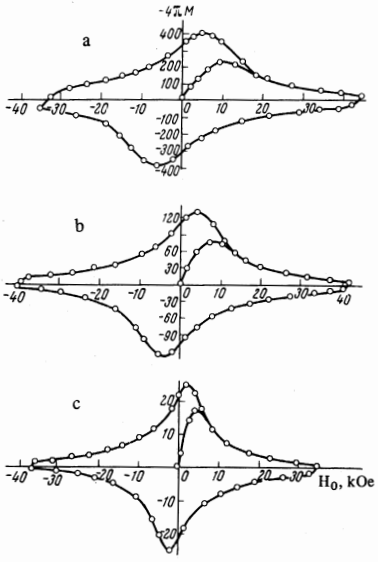


FIG. 2. Positions of the maxima on the $M(H_0)$ curves vs. the sample radius: a–sample 1, R = 0.33 mm; b–sample 2, R = 0.225 mm; c–sample 3, R = 0.125 mm. Sample 1 was prepared by cold deformation followed by aging for one hour at T = 425°C. Samples 2 and 3 were obtained from sample 1 by etching in a mixture of sulfuric and nitric acid.

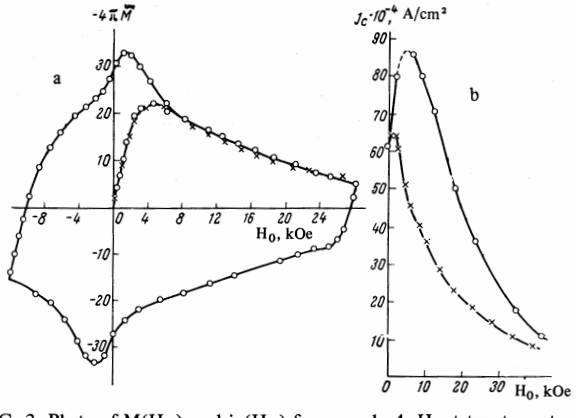


FIG. 3. Plots of $M(H_0)$ and $j_c(H_0)$ for sample 4. Heat treatment: recrystallization at 800°C for one hour followed by aging at 390°C for ten hours. T = 4.2° K. a–M in arbitrary units, X–theory, O–experiment; b–experiment, O–$j_c \parallel H_0$, X–$j_c \perp H_0$.

## 3. THE RATIO $H_{c3}/H_{c2}$ AND THE PARAMAGNETIC EFFECT

The equations of the Ginzburg-Landau theory do not take into account the interaction of the electron spin with the external magnetic field $H_0$ (the Pauli paramagnetism). In alloys with high values of $H_{c2}$ and $H_{c3}$, however, the paramagnetism of the electron gas may exert a strong influence on the destruction of superconductivity. As shown by Glogston, at T = 0, in fields exceeding

$$H_p(0) = 18\,400\, T_c \quad (17)$$

the superconducting state is not realized[8]. A measure of the influence of paramagnetism on $H_{c2}(0)$ is the coefficient

$$\alpha = \sqrt{2} H_{c2}^*(0) / H_p(0), \quad (18)$$

where

$$H_{c2}^*(0) = 2{,}58 \cdot 10^4 \rho_n \gamma T_c \quad (19)$$

is the upper critical field, calculated by Gor'kov under

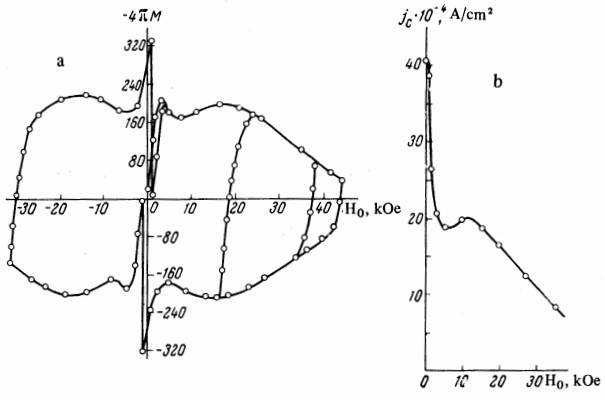


FIG. 4. Plots of $M(H_0)$ and $j_{c\perp}(H_0)$ for sample 5. Heat treatment: recrystallization at t = 800°C for one hour, followed by aging at t = 390°C for one hour. T = 4.2° K. a–M in arbitrary units, b–points $j_c \perp H_0$.

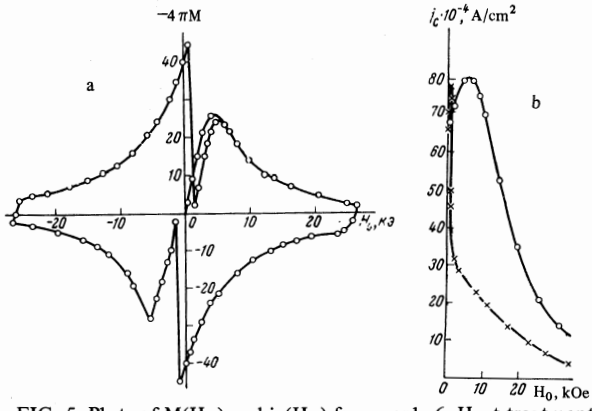


FIG. 5. Plots of $M(H_0)$ and $j_c(H_0)$ for sample 6. Heat treatment: recrystallization at 800°C for one hour, followed by aging at 425°C for ten hours. T = 4.2°K. a–M in arbitrary units; b–O–$j_c \parallel H_0$, X–$j_c \perp H_0$.

the assumption that there are no paramagnetic effects[8]; $\rho_n$ is the resistivity near $T_c$ in ohm-cm, and $\gamma$ is the coefficient of the linear term of the specific heat, in erg/cm$^3$—°K$^2$.

Saint-James and Sarma[9,10] have shown that near $T_c$ we have

$$\Theta = \frac{H_{c3}(T_c)}{H_{c2}(T_c)} = \frac{\{1+2(1,7\alpha)^2\}^{1/2}-1}{1.7\,\{(1+2\alpha^2)^{1/2}-1\}}. \quad (20)$$

Thus, $\Theta$ depends on the paramagnetic effect and tends to unity at large $\alpha$.

The influence of paramagnetism of electrons on $\Theta$ was investigated by us on samples 5 and 7. The measurements were made near $T_c$. The results are shown in Fig. 6 and in the table.

For sample 5, the measured value of $\Theta(T_c)$ is 1.38. Substituting it in (20), we get $\alpha_1 = 0.95$. On the other hand, knowing that $\rho_n$ of sample 5 amounts to $1.03 \times 10^{-4}$ ohm-cm, and $\gamma = 7.65 \times 10^3$ erg/cm$^3$—°K$^2$, we find from formula (8) that $\alpha_2 = 1.52$. The lower value of $\alpha_1$ obtained from direct measurements of the superconducting properties indicates that the paramagnetic effect is weaker than that expected from formula (18). A similar conclusion is obtained by substituting the value $\alpha_2 = 1.52$ in the Maki formula[10] for $H_{c2}(0)$:

$$H_{c2}(0) = \frac{H_{c2}^*(0)}{(1+\alpha^2)^{1/2}}. \quad (21)$$

Here $\alpha$ and $H^*_{c2}(0)$ are described by expressions (18) and (19). The value of $H_{c2}(0)$ for sample 5, calculated in formula (21), is 75 kOe, whereas extrapolations of the experimental data to zero temperature yields 84 kOe. The weakening of the paramagnetic effect is apparently connected with the presence of spin-orbit scattering, which brings closer together the values of the paramagnetic susceptibility of the normal and superconducting phases[8].

In sample 7, the paramagnetic effect is stronger than in sample 5, and it has $\Theta(T_c) = 1.2$. This result agrees with the data of[11], according to which the paramagnetic effect in the Ti-Nb system in the Nb concentration range 20—30 at.% becomes stronger with increasing concentration of Nb (sample 7 was annealed three hours at 450°C, and sample 5 for one hour at t = 380°C, therefore the matrix of sample 7 was much richer in niobium than the matrix of sample 5).

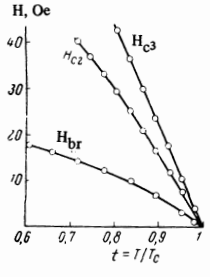


FIG. 6. Sample 5. Plots of $H_{c2}$, $H_{c3}$, and $H_{br}$ against $t = T/T_c$, $H_{br}$—value of the external field corresponding to breakdown of the superconductivity of the $\omega$ particles (to the maximum on the $M(H_0)$ and $j_c \perp (H_0)$ curves of Fig. 4).

## 4. PROXIMITY EFFECT

The proximity effect is called the interaction between a superconductor with nonsuperconducting metal in the presence of an interface. In alloys with small mean free paths, containing nonsuperconducting inclusions ($\omega$ and $\alpha$ particles in the Ti-Nb system), the superconducting pairs diffuse in the normal metal, inducing in it superconductivity at distances on the order of the coherence length $\xi(T)$. The action of the proximity effect on the properties of the $\omega$ and $\alpha$ particles should be strongest when the dimensions of the particles are of the order of $\xi(T)$, and the compositions of the matrix and of the inclusions are close to each other.

In order to verify this assumption, we investigated the temperature dependence of the magnetization of sample 5, which has a "peak effect"[3] (see Fig. 4). The dimensions of the semiaxis of the $\omega$ ellipsoids of sample 5, according to data obtained by transmission electron microscopy, are 45 × 125 Å at a coherence length

$$\xi(T) = 48(1-t^2)^{-1/2}\ \text{Å}, \quad (22)$$

while the composition of the $\omega$ phase is close to the composition of the matrix. The results were compared with the temperature variation of $j_{c\perp}(H_0)$, obtained for sample 4[12], in which the dimensions of the semiaxes of the $\omega$ ellipsoids reach 80 × 225 Å, and $\xi(0) = 40$ Å, and on sample 8 (semiaxes 82 × 120 Å, $\xi(0) \approx 42$ Å). In both samples, the composition of the $\omega$ phase is close to 17% Nb in Ti. Sample 4 at $T > 4.0$°K, and sample 8 at $T > 3.6$°K have a rigid vortex lattice[3] in the entire region $H_{c_1} < H_0 < H_{c2}$.

At lower temperatures, when $T < T_c(\omega)$, the $\omega$ ellipsoids go over into the superconducting state, and a peak corresponding to their breakdown (to the transition to the normal state) appears on the $j_{c\perp}(H)$ curves. With further lowering of the temperature, the peak shifts towards larger external magnetic field intensities[12].

The results obtained with sample 5 are shown in Fig. 6 in the form of a plot of $H_{c2}(\mathcal{M})$ and $H_{br} = H_{c2}(\omega)$ against the reduced temperature. Here $H_{c2}(\mathcal{M})$ is the second critical field of sample $\mathcal{M}$ (the matrix), and $H_{c2}(\omega)$ is the value of the field corresponding to the position of the maximum ("peak effect") on the $\mathcal{M}(H_0)$ curve. It turns out that $H_{c2}(\mathcal{M})$ depends linearly on $t^2$, whereas $H_{br}$ grows much more slowly with decreasing temperature. We note that the "peak effect" is retained down to temperatures close to $T_c(\mathcal{M})$, i.e.,

| Sample 5, $T_c = 6.92$° K | | | | Sample 7, $T_c = 7.72$° K | | | |
|---|---|---|---|---|---|---|---|
| $t = T/T_c$ | $H_{c2}$, kOe | $H_{c3}$, kOe | $\Theta$ | $t = T/T_c$ | $H_{c2}$, kOe | $H_{c3}$, kOe | $\Theta$ |
| 0,95 | 7,4 | 10,4 | 1,40 | 0,96 | 8,9 | 10,6 | 1,19 |
| 0,92 | 11,9 | 16,8 | 1,41 | 0,92 | 18,2 | 21,6 | 1,19 |
| 0,90 | 16,3 | 23,3 | 1,43 | 0,90 | 22,3 | 26,7 | 1,20 |
| 0,87 | 20,8 | 29,9 | 1,44 | 0,88 | 26,3 | 32,2 | 1,22 |
| 0,84 | 25,1 | 36,5 | 1,45 | 0,86 | 30,1 | 37,1 | 1,23 |
| 0,80 | 30,1 | 45 | 1,46 | 0,84 | 33,7 | 41,8 | 1,24 |

$$T_c(\mathcal{M}) \approx T_c(\omega). \quad (23)$$

The samples 4 and 8 behave differently. First, their $T_c(\mathcal{M})$ is much lower than $T_c(\omega)$ (for example, for sample 8 we have $T_c(\omega) \approx 3.7°K$ whereas $T_c(\mathcal{M}) = 8.62°K$). Second, the dependence of $H_{br}$ on $t^2$ is linear.

In comparing the behavior of samples 5, 4, and 8 one can see clearly the action of the proximity effect. In sample 5, the minor semiaxes of the $\omega$ particles are comparable in magnitude with $\xi(T)$, and therefore the superconducting pairs of the matrix induce in them superconductivity and induced superconductivity exists in the entire temperature interval $0 \leq T \leq T_c(\mathcal{M})$. In samples 4 and 8 the dimensions of the semiaxis exceed $\xi(T)$ (with the exception of the narrow region near $T_c$) and the superconductivity is induced only in the shell of the $\omega$ ellipsoids, which has a thickness $\xi(T)$. Thus, in these samples the matrix practically does not act on the core of the $\omega$ particles and the superconducting properties of the core are true properties of the $\omega$ phase of the given composition, not masked by the proximity effect. Therefore $T_c(\omega) < T_c(\mathcal{M})$ and $H_{c_2}(\omega)$ increases quadratically with decreasing temperature.

The authors thank B. M. Vul for interest in the work and valuable advice. The authors are grateful to A. I. Rusinov for a derivation of certain formulas, and also to Yu. F. Bychkov, V. A. Mal'tsev, M. T. Zuev, and I. A. Baranov for preparing the samples.

[1] C. P. Bean, Phys. Rev. Lett. 8, 250 (1962).
[2] A. D. McIntruff and A. Paskin, J. Appl. Phys. 40, 2431 (1969).
[3] Yu. F. Bychkov, V. G. Vereshchagin, V. R. Karasik, G. B. Kurganov, and V. A. Mal'tsev, Zh. Eksp. Teor. Fiz. 56, 505 (1969) [Sov. Phys.-JETP 29, 276 (1969)].
[4] V. V. Andrianov, V. B. Zenkevich, V. V. Sychev, V. I. Sokolov, L. F. Fedotov, and V. A. Tovma, Dokl. Akad. Nauk SSSR 169, 316 (1966) [Sov. Phys.-Dokl. 10, 1104 (1967)].
[5] S. Sh. Akhmedov, V. R. Karasik, and A. I. Rusinov, Zh. Eksp. Teor. Fiz. 56, 444 (1969) [Sov. Phys.-JETP 29, 243 (1969)].
[6] W. A. Fietz, M. R. Beasley, J. Silcox, and W. W. Webb, Phys. Rev. 136A, 335 (1964).
[7] P. DeGennes, Superconductivity of Metals and Alloys, Benjamin, 1965.
[8] D. Saint-James, G. Sarma, and E. J. Thomas, Type II Supercond., Pergamon Press, London, 1969.
[9] D. Saint-James and G. Sarma, Conf. on the Phys. of Type II Superconductivity, Cleveland, Ohio, USA, August 28, 1964.
[10] Y. B. Kim, C. F. Hempstead, and A. R. Strnad, Phys. Rev. 139A, 1163 (1965).
[11] T. G. Berlincourt and R. R. Hake, Phys. Rev. Lett. 9, 293 (1962).
[12] V. R. Karasik, V. G. Vereshchagin, and G. T. Nikitina, Kratkie soobshcheniya po fizike (Brief Physics Reports), FIAN, No. 5, 1970.

Translated by J. G. Adashko
92